

Solvation of Uranyl(II), Europium(III) and Europium(II) Cations in Basic Room-Temperature Ionic Liquids: A Theoretical Study

Alain Chaumont and Georges Wipff^{*,[a]}

Abstract: We report a molecular dynamics study of the solvation of UO_2^{2+} , Eu^{3+} and Eu^{2+} ions in two “basic” (Lewis acidity) room-temperature ionic liquids (IL) composed of the 1-ethyl-3-methylimidazolium cation (EMI^+) and a mixture of AlCl_4^- and Cl^- anions, in which the $\text{Cl}^-/\text{AlCl}_4^-$ ratio is about 1 and 3, respectively. The study reveals the importance of the $[\text{UO}_2\text{Cl}_4]^{2-}$ species, which spontaneously form during most simulations, and that the first solvation shell of europium is filled with Cl^- and AlCl_4^- ions embedded in a cationic EMI^+ shell. The stability of the

$[\text{UO}_2\text{Cl}_4]^{2-}$ and $[\text{Eu}^{\text{III}}\text{Cl}_6]^{3-}$ complexes is supported by quantum mechanical calculations, according to which the uranyl and europium cations intrinsically prefer Cl^- to the AlCl_4^- ion. In the gas phase, however, $[\text{Eu}^{\text{III}}\text{Cl}_6]^{3-}$ and $[\text{Eu}^{\text{II}}\text{Cl}_6]^{4-}$ complexes are predicted to be metastable and to lose two to three Cl^- ions. This contrasts with the results of simulations of complexes in ILs, in

which the “solvation” of the europium complexes increases with the number of coordinated chlorides, leading to an equilibrium between different chloro species. The behavior of the hydrated $[\text{Eu}(\text{OH}_2)_8]^{3+}$ complex is considered in the basic liquids; the complex exchanges H_2O molecules with Cl^- ions to form mixed $[\text{EuCl}_3(\text{OH}_2)_4]$ and $[\text{EuCl}_4(\text{OH}_2)_3]^-$ complexes. The results of the simulations allow us to better understand the microscopic nature and solvation of lanthanide and actinide complexes in “basic” ionic liquids.

Keywords: europium • green chemistry • ionic liquids • molecular dynamics • solvent effects

Introduction

The mixing of anhydrous aluminium chloride with chloride salts of certain quaternary ammonium cations (e.g., alkylpyridinium, -guanidinium, or -imidazolium; see Figure 1) produces molten salts that are liquid at ambient tempera-

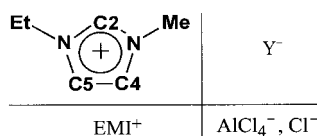


Figure 1. Ionic components of the imidazolium-based ILs used for the MD simulations with atom labels and charges. The tetrachloroaluminate AlCl_4^- anion will be denoted as “TCA⁻” (solvent component) or “tca⁻” (uranyl or europium ligand).

ture.^[1–3] There is growing interest in such room-temperature ionic liquids (hereafter denoted as ILs) in the field of “green chemistry”, owing to their nonflammability, high thermal stability, and low vapor pressure. Other interesting

characteristics, in comparison with classical solvents, include high electrical conductivity, a wide electrochemical window, and the possibility of monitoring their solvation properties and “acidic”/“basic” Lewis character by changing the ratio of the different components of the ILs. Melts prepared from an excess of AlCl_3 contain unsaturated species such as Al_2Cl_7^- and are “acidic”, while those containing an excess of the organic chloride salt are “basic”. Basic melts prepared from AlCl_3 /ethylmethylimidazolium chloride have been shown to be excellent solvents for anionic chloride complexes with d and f elements, presumably because these complexes are well solvated by the IL; this prevents solvolysis decomposition reactions. ILs may also be used to mimic the solvation of inorganic cations in high-temperature molten salts (e.g., $\text{AlCl}_3\text{-NaCl}$ or LiCl-KCl).^[4–5] Electrochemical studies of lanthanide and actinide cation complexes (e.g., $[\text{UCl}_6]^{3-}$, $[\text{UO}_2\text{Cl}_4]^{2-}$, $[\text{SmCl}_6]^{3-}$, or $[\text{CeCl}_6]^{3-}$, $[\text{NpCl}_6]^{3-}$) in chloroaluminate melts have been reported^[6–9] and have potential applications in the field of nuclear fuel reprocessing.^[10] Other studies have focused on the dissolution and liquid–liquid extraction of metals and f elements in ILs that are immiscible with water.^[11–14]

Little is known about the microscopic structures of such ILs in terms of their composition, or about their solvation properties with respect to metallic ions. This led our group to initiate molecular dynamics (MD) studies on solutions

[a] A. Chaumont, Prof. G. Wipff
Laboratoire MSM, UMR CNRS 7551, Institut de Chimie
4 rue B. Pascal, 67 000 Strasbourg (France)
Fax: (+33)3-90-24-15-45
E-mail: wipff@chimie.u-strasbg.fr

with prototypal ions that need to be separated from nuclear wastes. Following the simulations reported by others on neat liquids^[15–18] and on their solvation properties with respect to small organic molecules,^[19–21] we investigated the solvation of UO_2^{2+} , Sr^{2+} , and M^{3+} lanthanide ($\text{M}=\text{La}/\text{Eu}/\text{Yb}$) cations in two ILs: [BMI][PF₆] (1-butyl-3-methylimidazolium PF₆[−]) and [EMI][TCA] (1-ethyl-3-methylimidazolium tetrachloroaluminate[−]).^[22,23] These studies showed how the anionic components of the ILs solvate the di- and trivalent cations with different coordination numbers, binding modes, and dynamic features depending on the size, charge, and shape of the cation. These two liquids were “neutral”, but it has been observed experimentally that cations dissolve less well in these ILs than in basic liquids.^[24] The solvation of uranyl [UO_2Cl_n]^{2−*n*} ($n=2–4$) and lanthanide [MCl_m]^{3−*m*} ($m=3–8$) complexes has been recently studied by molecular dynamics in the neutral [EMI][TCA] and [BMI][PF₆] ionic liquids; these studies showed that the TCA[−] or PF₆[−] solvent anions coordinated to the unsaturated complexes.^[25] We thus decided to extend our investigations to basic ILs containing Cl[−] ions. For this purpose, we compared two liquids based on [EMI][*x*TCA,*y*Cl]_{*R*} containing a mixture of TCA[−] and Cl[−] ions; this formally corresponds to the reaction of (*x*+*y*) moles of the EMI⁺Cl[−] salt with *x* moles of AlCl₃. These will be denoted as IL_{*R*}, in which *R* is the approximate *y/x* ratio, that is, *R*=1 or 3. The exact compositions of the IL₁ and IL₃ liquids and their solutions are given in Table 1. As solutes, we considered the UO_2^{2+} ion, which is of the utmost impor-

the solvation of the uranyl and europium cations in these basic ILs and the neutral [EMI][TCA] liquid. The simulated systems were “dry”. However, given the high hygroscopic character of the solutes, we have also investigated the behavior of the $[\text{Eu}(\text{OH}_2)_8]^{3+}$ complex in both liquids, in which water and chloride ions compete to bind to the cation. The molecular dynamics studies are complemented by quantum mechanical investigations of selected uranyl and europium complexes in the gas phase.

Computational Methods

Molecular dynamics: The systems were simulated by classical molecular dynamics (MD) by using the modified AMBER 5.0 software^[26] in which the potential energy (*U*) is described by the sum of the bond, angle, and dihedral deformation energies and pair-wise additive 1–6–12 (electrostatic and van de Waals) interactions between nonbonded atoms [Eq. (1)].

$$U = \sum_{\text{bonds}} k_b(b-b_0)^2 + \sum_{\text{angles}} k_\theta(\theta-\theta_0)^2 + \sum_{\text{dihedrals}} \sum_n V_n[1 + \cos(n\varphi-\gamma)] + \sum_{i < j} \left[\frac{q_i q_j}{R_{ij}} - 2\epsilon_{ij} \left(\frac{R_{ij}^*}{R_{ij}} \right)^6 + \epsilon_{ij} \left(\frac{R_{ij}^*}{R_{ij}} \right)^{12} \right] \quad (1)$$

Cross terms of van der Waals interactions were constructed by using the Lorentz–Berthelot rules. The EMI⁺ and TCA[−] ion parameters used for the ILs were taken from the work of Stassen et al. and have been tested on the properties of the pure liquids.^[16,22] The van der Waals parameters for UO_2^{2+} ($R_{\text{UO}_2}^*=1.58 \text{ \AA}$; $\epsilon_{\text{UO}_2}=0.4 \text{ kcal mol}^{-1}$)^[27] and Eu^{3+} ($R_{\text{Eu}}^*=1.852 \text{ \AA}$; $\epsilon_{\text{Eu}}=0.05 \text{ kcal mol}^{-1}$)^[28] were fitted to the free energies of hydration. The parameters used for the Eu^{2+} ion were those determined for Sr^{2+} ($R^*=1.7412 \text{ \AA}$, $\epsilon=0.1182 \text{ kcal mol}^{-1}$)^[29] which has a similar ionic radius (1.17 versus 1.18 Å, respectively, for a six-coordinate complex and 1.25 versus 1.26 Å, respectively, for an eight-coordinate complex^[30,31]). For the Cl[−] ions, we used the parameters ($R^*=2.495 \text{ \AA}$, $\epsilon=0.107 \text{ kcal mol}^{-1}$) developed from the free energies of hydration.^[32] The 1–4 van der Waals interactions were scaled down by a factor of 2.0 and the 1–4 coulombic interactions were scaled down by 1.2. The solutions were simulated with 3D-periodic boundary conditions. Nonbonding interactions were calculated with a 12 Å atom-based cut-off, and corrected for long-range electrostatic interactions by using the Ewald summation method (PME approximation).^[33]

The MD simulations of the uranyl or europium solutions were performed at 400 K starting with random velocities. The temperature was monitored by coupling the system to a thermal bath by using the Berendsen algorithm^[34] with a relaxation time of 0.2 ps. All C–H bonds were constrained with SHAKE, using the Verlet leapfrog algorithm with a time step of 2 fs to integrate the equations of motion.

We first equilibrated “cubic” boxes of pure solvents by repeated sequences of 1) heating the system at 500 K at constant volume for 0.5 ns, followed by 2) 0.5 ns of dynamics at 300 K and a constant pressure of 1 atm, and 3) 1 ns of dynamics at 300 K and constant volume. The final box was simulated for 1 to 5 ns at 400 K (see Table 1).

The uranyl or europium ions were immersed in a given IL, while EMI⁺ solvent ions were removed to maintain the neutrality of the box. The solvent boxes with a single metal ion are cubic ($\approx 44 \text{ \AA}$ in length) and contain ≈ 300 EMI⁺ ions and ≈ 150 TCA[−] + 150 Cl[−] ions (IL₁) or ≈ 75 TCA[−] + 225 Cl[−] ions (IL₃). More concentrated solutions of europium and uranyl ions (with nine cations per box) were also simulated with larger boxes. Details are given in Table 1.

Equilibration started with 1500 steps of steepest descent energy minimization, followed by 50 ps of MD with fixed solutes (the “BELLY” option of AMBER) at constant volume and by 50 ps without constraints, followed by 50 ps at a constant pressure of 1 atm. Subsequent MD trajectories were run for 1.5–5 ns and saved every 0.5 ps. Sampling tests were performed based on mixing–demixing simulations. The mixing was obtained

Table 1. Characteristics of the simulated systems and simulation conditions.

| System | EMI ⁺ | TCA [−] | Cl [−] | Box size [Å ³] | <i>t</i> [ns] |
|---|------------------|------------------|-----------------|----------------------------|---------------|
| pure IL ₁ | 304 | 152 | 152 | 44.5 | 1.5 |
| pure IL ₃ | 304 | 76 | 228 | 43.4 | 1 |
| UO_2^{2+} in IL ₁ | 298 | 150 | 150 | 44.5 | 2 |
| UO_2^{2+} in IL ₃ | 298 | 75 | 225 | 43.4 | 1.5 |
| 9 UO_2^{2+} in IL ₁ | 700 | 359 | 359 | 59.3 | 2 |
| Eu^{2+} in IL ₁ | 296 | 149 | 149 | 44.3 | 4 |
| [EuCl ₆] ^{4−} in IL ₁ | 292 | 147 | 141 | 44.1 | 1.5 |
| 9 Eu^{2+} in IL ₁ | 700 | 359 | 359 | 59.2 | 2 |
| Eu^{2+} in IL ₃ | 294 | 74 | 222 | 44.2 | 1.5 |
| [EuCl ₆] ^{4−} in IL ₃ | 294 | 74 | 216 | 43.6 | 1.5 |
| 9 Eu^{2+} in IL ₃ | 602 | 155 | 465 | 54.7 | 2 |
| Eu^{3+} in IL ₁ | 291 | 147 | 147 | 44.2 | 5 |
| [EuCl ₆] ^{3−} in IL ₁ | 291 | 147 | 141 | 44.0 | 1.5 |
| [Eu(H ₂ O) ₈] ³⁺ in IL ₁ | 291 | 147 | 147 | 44.1 | 5 |
| 9 Eu^{3+} in IL ₁ | 700 | 363 | 364 | 59.4 | 2 |
| Eu^{3+} in IL ₃ | 293 | 74 | 222 | 43.4 | 4.5 |
| [EuCl ₆] ^{3−} in IL ₃ | 296 | 72 | 221 | 43.1 | 1.5 |
| [Eu(H ₂ O) ₈] ³⁺ in IL ₃ | 293 | 74 | 222 | 43.0 | 5 |
| 9 Eu^{3+} in IL ₃ | 600 | 159 | 468 | 55.8 | 2 |

tance in the nuclear industry, and Eu^{3+} , which represents an average-sized lanthanide and is a good model for trivalent actinides such as Am^{3+} . The divalent Eu^{2+} state of europium was also considered for comparison. We investigated the coordination of the solvent anions, Cl[−] and TCA[−], to the cation at two Cl[−] concentrations (IL₁ vs IL₃) and compared

by 0.5 ns of MD at 600 K with biased potentials (electrostatics scaled down by a factor of 100), while the subsequent demixing was achieved by resetting the original electrostatics and by stepwise cooling ($\Delta T = -25$ K per 25 ps of MD at each step) of the system to 400 K.

The trajectories were analyzed with the MDS and DRAW software.^[35] The average solvation structure was characterized by the radial distribution functions (RDFs) of the Al, Cl, and N_{ethyl} (EMI^+) atoms of the solvent around the U_{O_2} or Eu atoms during the last 0.2 ns of MD. Insights into the energy components were obtained by group analysis using a 17 Å cut-off distance and a reaction field correction for the electrostatics.^[36] Typical snapshots were redrawn with VMD.^[37]

Quantum mechanics calculations: The $[\text{EuCl}_4(\text{tca})_2]^{3-}$, $[\text{EuCl}_n]^{3-n}$, $[\text{UO}_2\text{Cl}_2(\text{tca})_2]^{2-}$, $[\text{UO}_2\text{Cl}_3(\text{tca})]^{2-}$ and $[\text{UO}_2\text{Cl}_4]^{2-}$ complexes were optimized without symmetry constraints by quantum mechanical (QM) calculations at the Hartree–Fock (HF) and DFT (B3LYP functional) levels of theory, using the Gaussian 98 software.^[38] The H, C, N, O, and Cl atoms were described by the 6-31+G* basis set.^[38] For uranium, we used the relativistic large core effective core potential (ECP) of the Los Alamos group^[39] with 78 electrons in the core and a [3s,3p,2d,2f] contracted valence basis set. The 46 core and 4f electrons of the europium were similarly described by the large core ECP of the Stuttgart group^[40,41] complemented by the affiliated [5s,4p,3d] contracted basis set,^[42] enhanced by an additional f-function with an exponent of 0.591.

Results

We first describe the main characteristics of the neat IL_1 and IL_3 basic liquids and then examine the solvation of the uranyl and europium cations in each of them.

Characteristics of the neat basic liquids: The basic liquids were simulated at 400 K, and the calculated density of IL_1 (1.21 g cm^{-3}) is close to the experimental value (1.23 g cm^{-3} at 400 K),^[43] while for IL_3 (calculated density 1.11 g cm^{-3}) no experimental data are available. The average structures of the basic liquids and of the neutral $[\text{EMI}][\text{TCA}]$ liquid (without Cl^- ions) are characterized by the RDFs between EMI^+ and the Cl^- and AlCl_4^- ions (see Figure 2; the characteristics of the RDFs are summarized in Table 2). Unless otherwise specified, the N_{ethyl} atom was selected to define the EMI^+ distribution. In addition, the distribution of Cl^- ions around the C_2H , C_4H , and C_5H protons of EMI^+ was investigated. Figure 2 shows that the IL_1 and IL_3 liquids have qualitatively similar RDFs, which differ markedly from the RDF of the neutral liquid. The main difference is due to the Cl^- ions that coordinate to each EMI^+ ion more or less in-plane through the acidic C_2H , C_4H , and C_5H protons. Typical snapshots of the interacting ions are shown in Figure 3. The $\text{C}_2\text{H}\cdots\text{Cl}^-$ RDF (Figure 2) peaks at 3.0 Å and integration (up to 4.7 Å) indicates that the C_2H proton coordinates to 1.0 Cl^- ions in the IL_1 liquid and to 1.4 Cl^- anions in the IL_3 liquid. Similarly, the C_4H and C_5H protons coordinate on average to 0.7–0.8 Cl^- ions in IL_1 , and to 1.1–1.2 Cl^- ions in IL_3 . On average each Cl^- ion is surrounded by three to four EMI^+ ions (see also Figure 2). Similar interactions have been observed in the solid-state structure of BMI^+Cl^- , which has a short $\text{C}_2\text{H}\cdots\text{Cl}^-$ hydrogen bond (2.52 Å).^[44] These results are also consistent with those of the QM calculations^[45] and MD^[15,19] simulations of imidazolium chloride salts. According to our force field calculations on $\text{EMI}^+\cdots\text{Cl}^-$ dimers in the gas phase, the interaction at the C_2H

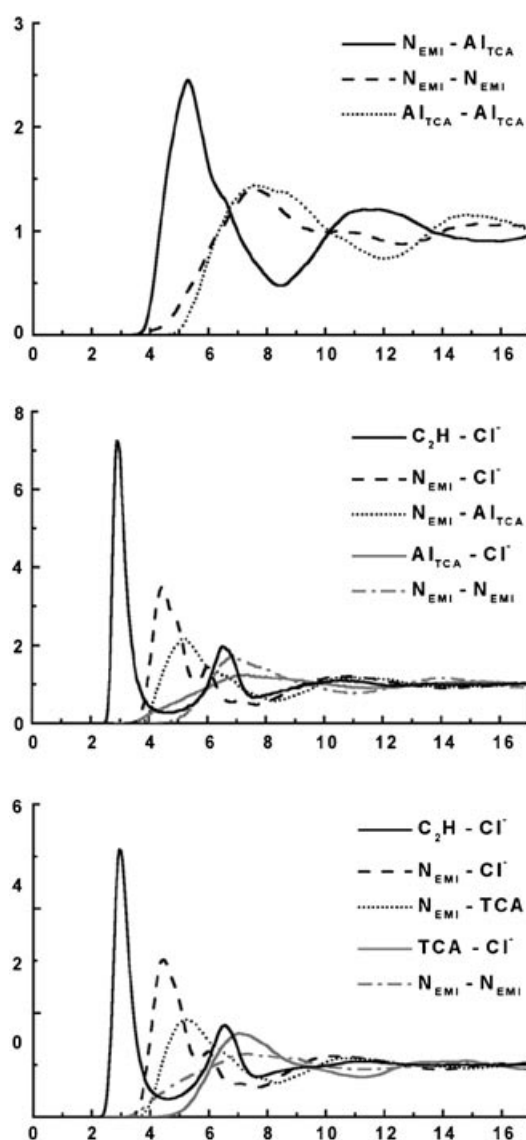


Figure 2. Pure neutral $[\text{EMI}][\text{TCA}]$ (top) and basic IL_1 (middle) and basic IL_3 (bottom) liquids: anion–anion, cation–cation, and anion–cation radial distribution functions as a function of distance [Å]. Averages over the last 200 ps. Typical snapshots are given in Figure 3.

($-86.9 \text{ kcal mol}^{-1}$) position is slightly favored over the C_4H or C_5H positions ($-84.4 \text{ kcal mol}^{-1}$), as in the quantum mechanically optimized structures.^[45]

The second important peak in the solvent RDFs is at ≈ 4.5 Å in the IL_1 and IL_3 liquids and corresponds to the $N_{\text{ethyl}}\cdots\text{Cl}^-$ pair. Integration (up to 7.7 Å) indicates that the N_{ethyl} atom coordinates to 3.4 Cl^- and to 5.3 Cl^- ions, respectively. The $\text{Cl}^-\cdots\text{EMI}^+$ distribution in these liquids thus resembles the Cl^- distribution in the 1,3-dimethylimidazolium chloride liquid that was studied by neutron diffraction.^[46] There is a broad $\text{EMI}^+\cdots\text{TCA}^-$ peak at about 5.3 Å, as in the neutral $[\text{EMI}][\text{TCA}]$ liquid, but this peak is less pronounced in the basic liquids due to the lower concentration of TCA^- ions. The peak is smaller in IL_3 than in IL_1 (2.1 versus 4.1 TCA^- ions) for the same reason. Some TCA^- ions are surrounded by up to three EMI^+ ions (see

Table 2. Characteristics of the first peaks in the solvent RDFs of pure IL₁ and IL₃ at 400 K: integration of the first peak (first line) and distances [Å] of the first maximum and minimum (second line). Averages over the last 0.2 ns of MD. Atom labels are shown in Figure 1.

| | IL ₁ | IL ₃ |
|--|-------------------|-------------------|
| N1 _{EMI} ...Cl | 3.4 4.5; 7.7 | 5.3 4.5; 7.6 |
| Cl...N1 _{EMI} | 3.6 4.5; 5.6 | 3.9 4.5; 5.6 |
| H2 _{EMI} ...Cl | 1.0 3.0; 4.7 | 1.4 3.0; 4.6 |
| Cl...H2 _{EMI} | 1.9 3.0; 4.7 | 1.9 3.0; 4.7 |
| H4 _{EMI} ...Cl | 0.8 3.0; 4.4 | 1.2 3.0; 4.4 |
| Cl...H4 _{EMI} | 1.6 3.0; 4.4 | 1.8 3.0; 4.4 |
| H5 _{EMI} ...Cl | 0.7 3.0; 4.4 | 1.1 3.0; 4.4 |
| Cl...H5 _{EMI} | 1.5 3.0; 4.4 | 1.5 3.0; 4.4 |
| N1 _{EMI} ...Al _{TCA} | 4.1 5.3; 8.3 | 2.1 5.2; 8.2 |
| Al _{TCA} ...N1 _{EMI} | 8.2 5.3; 8.3 | 8.1 5.3; 8.3 |
| N1 _{EMI} ...N1 _{EMI} | 19.8 7.1; 11.3 | 22.7 7.6; 11.5 |
| Cl...Al _{TCA} | 9.7 7.1; 11.2 | 5.2 7.1; 11.2 |
| Cl...Cl | 7.5 6.0; 10.3 | 12.0 6.3; 10.1 |
| Al _{TCA} ...Al _{TCA} | 10.0 7.3; 11.5 | 5.3 7.1; 11.3 |

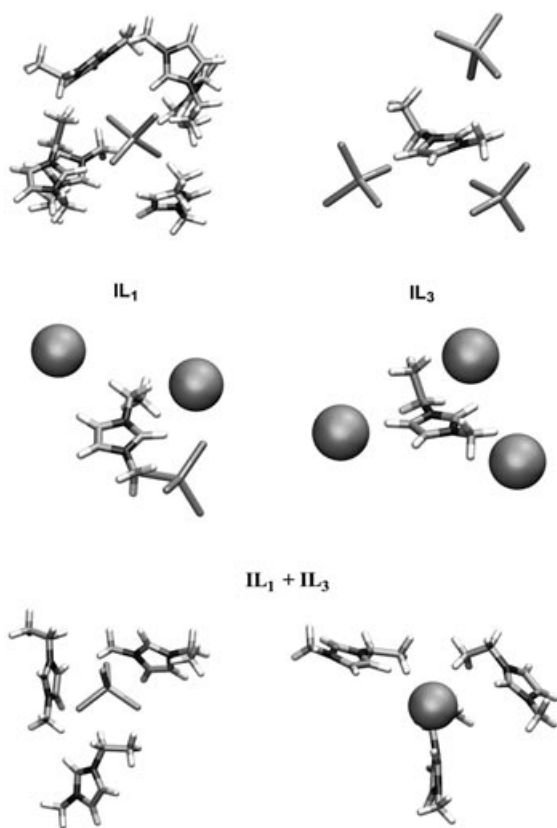


Figure 3. Pure neutral [EMI][TCA] and basic IL₁ and IL₃ liquids. Typical snapshots of the ions in interaction.

Figure 3); this sometimes leads to short contact distances between solvent anions.

An insight into the dynamics of the ionic components of the basic and neutral liquids was obtained from the diffusion coefficients (D) of the Cl⁻, N_{EMI+} and Al_{TCA-} atoms, calculated from the Stokes–Einstein equation [Eq. (2)].

$$6D(t) = \langle [r_i(t) - r_i(0)]^2 \rangle \quad (2)$$

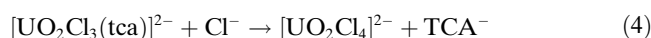
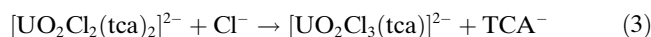
The average values over the last 1.5 ns of MD indicate reduced diffusion as the basicity of the liquid increases (i.e., neutral [EMI][TCA] > IL₁ > IL₃) for the EMI⁺ ions ($D = 1.04, 0.18, \text{ and } 0.02 \times 10^{-6} \text{ cm}^2 \text{ s}^{-1}$, respectively), the TCA⁻ ions ($D = 0.85, 0.09, \text{ and } 0.02 \times 10^{-6} \text{ cm}^2 \text{ s}^{-1}$, respectively) and Cl⁻ ions when present ($D = 0.08 \text{ and } 0.01 \times 10^{-6} \text{ cm}^2 \text{ s}^{-1}$, respectively). The value of $D(\text{EMI}^+)$ in the neutral liquid agrees well with the experimental value ($0.95 \times 10^{-6} \text{ cm}^2 \text{ s}^{-1}$),^[47] and the trends in the calculated diffusion values as the liquid becomes more basic are consistent with experiment.^[47] They are also consistent with the increased viscosity of the liquids and increased temperature of fusion of the corresponding solids as the Cl⁻ concentration increases.^[43] In a given liquid, the calculated ion diffusion decreases in the order $D(\text{EMI}^+) > D(\text{TCA}^-) > D(\text{Cl}^-)$.

The uranyl cation in the basic liquids: After immersion in the IL₁ basic liquid, the UO₂²⁺ ion rapidly (within 0.1 ns) captured anions from the solvent to form the mixed [UO₂Cl₃(tca)]²⁻ complex, which remained stable for 1.4 ns. Subsequent anion exchange with the solvent led to the [UO₂Cl₄]²⁻ complex, which was stable until the end of the dynamics (2 ns). Interestingly, the TCA⁻ ↔ Cl⁻ ligand exchange involved a Cl⁻ ion that was initially at about 10 Å from the uranyl species, and which diffused to the uranyl complex. The stability of this complex was further assessed by performing a mixing–demixing simulation; this also led to the formation of the mixed [UO₂Cl₃(tca)]²⁻ complex, which evolved in 0.23 ns to [UO₂Cl₄]²⁻ in which the uranyl is tetra-coordinated to Cl atoms at about 3 Å. A third sampling test was performed for 2 ns on a more concentrated IL₁ solution, with nine UO₂²⁺ ions in the solvent box. Initially there were five [UO₂Cl₃(tca)]²⁻ and four [UO₂Cl₂(tca)]²⁻ complexes and, after 2 ns, the solution contained a mixture of five [UO₂Cl₄]²⁻, two [UO₂Cl₃(tca)]²⁻, and two [UO₂Cl₂(tca)]²⁻ complexes. In the more basic IL₃ liquid, the uranyl cation immediately captured four chloride anions to form the [UO₂Cl₄]²⁻ complex and these remained bound until the end of the dynamics (1.5 ns). All these simulations suggest that in basic solvents [UO₂Cl₄]²⁻ is more stable and more abundant than mixed complexes such as [UO₂Cl₃(tca)]²⁻.

Further insight into the stability of the uranyl complexes comes from QM calculations performed on these complexes in the gas phase and from the analysis of solute–solvent interaction energies in the ionic liquids.

According to the QM calculations, the exchange of one TCA⁻ for one Cl⁻ ion [Eqs. (3) and (4)] is exothermic by -34.7 and $-20.6 \text{ kcal mol}^{-1}$, respectively (from DFT results), or by -33.3 and $-20.6 \text{ kcal mol}^{-1}$, respectively (from HF re-

sults). We note that our force-field calculations yield similar energies (-46.4 and -27.0 kcal mol $^{-1}$, respectively), which confirms that the competition between the different solvent anions is properly accounted for in the MD simulations.



The interaction energies of the $[\text{UO}_2\text{Cl}_4]^{2-}$ and $[\text{UO}_2\text{Cl}_3(\text{tca})]^{2-}$ complexes with the IL $_1$ solvent were also compared; the former complex is further stabilized by better solvation (by ≈ 35 kcal mol $^{-1}$, mainly due to reduced repulsion of the Cl^- solvent ions). Comparison of the interaction energy of UO_2^{2+} with its whole environment (i.e., coordinated and “free” solvent ions) also shows that the $[\text{UO}_2\text{Cl}_4]^{2-}$ complex interacts more strongly with the solvent than does the $[\text{UO}_2\text{Cl}_3(\text{tca})]^{2-}$ complex ($\Delta \approx -30$ kcal mol $^{-1}$; see Table 3).^[48]

The solvation of the negatively charged $[\text{UO}_2\text{Cl}_4]^{2-}$ complex in the two basic liquids was compared. Figure 4 shows typical snapshots of the first solvation shell around the U atom and the RDFs are given in Figure 5. The RDF characteristics are summarized in Table 4. The analysis confirms that the U atom is shielded from the solvent(s) by the four coordinated chloride anions. The tetrachloro complex is surrounded by a cage of eight to nine EMI $^+$ ions (within 10.0 Å), into which about two TCA $^-$ ions are inserted in an “axial” position with respect to the uranyl species. The similarity of the solvation patterns of $[\text{UO}_2\text{Cl}_4]^{2-}$ in IL $_1$ and IL $_3$ liquids was confirmed by an energy component analysis, according to which the interaction energies of the $[\text{UO}_2\text{Cl}_4]^{2-}$ complex and the corresponding UO_2^{2+} ion with the IL $_1$ and IL $_3$ liquids are also similar (see Tables 3 and 5).^[49]

The europium(III) cation in the IL $_1$ and IL $_3$ basic liquids: Simulation of the Eu^{3+} ion in the IL $_1$ liquid rapidly led to

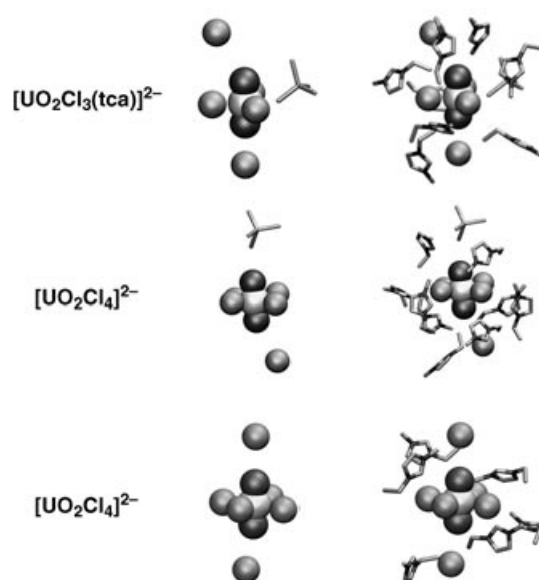


Figure 4. UO_2^{2+} in IL $_1$ (top and middle) and IL $_3$ (bottom) basic solutions: snapshots of the first solvation shell around the U atom with anions only (left) and anions + cations (right).

the formation of the $[\text{EuCl}_2(\text{tca})_3]^{2-}$ complex, in which two of the TCA $^-$ ions are bidentate; this corresponds to a total coordination number of seven for europium. After 75 ps, the complex captured a Cl^- ion to form $[\text{EuCl}_3(\text{tca})_3]^{3-}$ with three monodentate TCA $^-$ ions and then evolved to $[\text{EuCl}_4(\text{tca})_2]^{3-}$ (at 160 ps) and to $[\text{EuCl}_5(\text{tca})]^{3-}$ (at 1.7 ns). This last complex remained stable until the end of the dynamics (3.3 ns). Upon a subsequent mixing–demixing simulation, only the less chlorinated $[\text{EuCl}_3(\text{tca})_4]^{4-}$ was found to form (after 0.1 ns), and it remained stable for up to 2 ns. Another simulation on a more concentrated IL $_1$ solution with nine Eu^{3+} “naked” cations led, after 2 ns, to a mixture of three $[\text{EuCl}_3(\text{tca})_3]^{3-}$, three $[\text{EuCl}_4(\text{tca})_2]^{3-}$, and three

Table 3. Average interaction energies and fluctuations [kcal mol $^{-1}$] of the solutes with the IL $_1$ and IL $_3$ ionic liquids and their constitutive ions.

| System | EMI $^+$ | TCA $^-$ | Cl $^-$ | IL | EMI $^+$ | TCA $^-$ | Cl $^-$ | IL |
|--|-----------|-----------|-----------------------|------------|------------|----------|------------------------|-----------|
| | | | Cation ^[a] | | | | Complex ^[b] | |
| | | | | IL $_1$ | | | | |
| $[\text{UO}_2\text{Cl}_3(\text{tca})]^{2-}$ | 1242 (18) | -519 (15) | -1215 (17) | -492 (15) | -1355 (15) | 485 (14) | 649 (15) | -221 (12) |
| $[\text{UO}_2\text{Cl}_4]^{2-}$ | 1248 (22) | -487 (13) | -1287 (21) | -526 (16) | -1340 (20) | 524 (11) | 559 (15) | -257 (15) |
| $[\text{Eu}^{\text{II}}\text{Cl}_4(\text{tca})_2]^{4-}$ | 1284 (17) | -665 (14) | -1124 (19) | -505 (14) | -2763 (30) | 765 (20) | 1300 (30) | -667 (22) |
| $[\text{Eu}^{\text{II}}\text{Cl}_6]^{4-}$ | 1399 (18) | -378 (12) | -1626 (18) | -604 (16) | -2877 (30) | 820 (26) | 917 (30) | -838 (23) |
| $[\text{Eu}^{\text{III}}\text{Cl}_4(\text{tca})_2]^{3-}$ | 1862 (27) | -913 (19) | -2045 (24) | -1096 (22) | -2028 (23) | 670 (19) | 942 (21) | -415 (17) |
| $[\text{Eu}^{\text{III}}\text{Cl}_3(\text{tca})]^{3-}$ | 1866 (24) | -847 (25) | -2167 (31) | -1148 (21) | -2001 (21) | 747 (22) | 811 (29) | -443 (16) |
| $[\text{Eu}^{\text{III}}\text{Cl}_6]^{3-}$ | 2048 (29) | -566 (15) | -2691 (26) | -1208 (23) | -2146 (27) | 620 (14) | 1082 (33) | -487 (17) |
| | | | | IL $_3$ | | | | |
| $[\text{UO}_2\text{Cl}_4]^{2-}$ | 1293 (20) | -203 (13) | -1612 (22) | -522 (13) | -1389 (18) | 230 (13) | 915 (19) | -243 (13) |
| $[\text{Eu}^{\text{II}}\text{Cl}_3(\text{tca})_3]^{4-}$ | 1175 (21) | -549 (12) | -1140 (19) | -514 (16) | -2581 (37) | 498 (19) | 1427 (33) | -655 (21) |
| $[\text{Eu}^{\text{II}}\text{Cl}_5]^{4-}$ | 1285 (27) | -257 (17) | -686 (27) | -551 (18) | -2016 (34) | 397 (21) | 1120 (35) | -499 (19) |
| $[\text{Eu}^{\text{II}}\text{Cl}_6]^{4-}$ | 1377 (20) | -295 (9) | -1687 (20) | -605 (16) | -2845 (37) | 627 (19) | 1082 (33) | -833 (21) |
| $[\text{Eu}^{\text{III}}\text{Cl}_4(\text{tca})_2]^{3-}$ | 1650 (36) | -747 (31) | -1981 (39) | -1078 (23) | -1830 (31) | 453 (22) | 972 (27) | -404 (17) |
| $[\text{Eu}^{\text{III}}\text{Cl}_6]^{3-}$ | 2039 (26) | -361 (12) | -2890 (25) | -1212 (21) | -2147 (24) | 394 (11) | 1272 (21) | -479 (17) |

[a] Interaction between the uranyl or europium species and their whole environment (including first shell anions). [b] Interactions between the negatively charged “complex” (as defined in the first column) and the solvent.

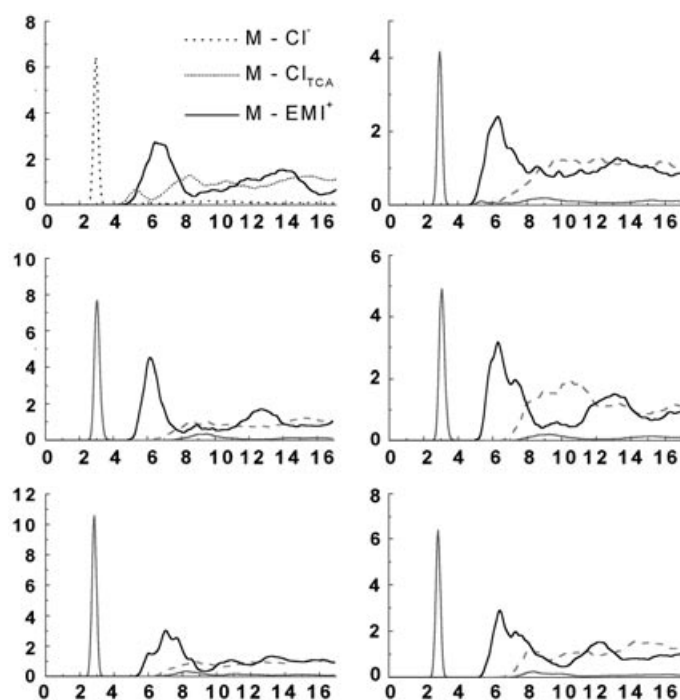


Figure 5. Solvent RDFs around the uranium or europium atom of $[\text{UO}_2\text{Cl}_4]^{2-}$ (top), $[\text{Eu}^{\text{IIICl}_6}]^{4+}$ (middle), and $[\text{Eu}^{\text{IIICl}_6}]^{3-}$ (bottom) complexes as a function of distance [Å]. Left: IL_1 , Right: IL_3 .

Table 4. Uranyl and europium salts in the IL_1 and IL_3 solutions: characteristics of the first peak of the radial distribution functions.

| System | IL_1 | | | IL_3 | | |
|-------------------------------------|---------------|----------------------------|------------------|---------------|----------------------------|-------------------|
| | Cl^- | Cl_{TCA}^- | EMI^+ | Cl^- | Cl_{TCA}^- | EMI^+ |
| $[\text{UO}_2\text{Cl}_4]^{2-}$ | 4 3; 3.6 | 1.8 5.3; 6.2 | 10.8 6.4; 8.7 | 4 3.0; 3.7 | 5.5 8.5; 9.3 | 13.9 6.4; 9.7 |
| $[\text{Eu}^{\text{IIICl}_6}]^{4+}$ | 6 3.1; 4.1 | 9.2 8.7; 9.1 | 10.4 6.2; 8.2 | 6 3.1; 4.0 | 10.5 9.0; 9.7 | 12.3 6.3; 8.8 |
| $[\text{Eu}^{\text{IIICl}_6}]^{3-}$ | 6 2.9; 3.5 | 17.7 8.8; 10.4 | 13.9 7.0; 9.4 | 6 2.9; 3.5 | 6 8.2; 9.3 | 16.4 6.4; 10.1 |

Table 5. Average interaction energies and fluctuations [kcal mol^{-1}] of the uranyl and europium chloro complexes with the IL_1 and IL_3 ionic liquids and their constitutive ions. TCA^- ions also involve anions that are coordinated to the metal, in the case of $[\text{UO}_2\text{Cl}_3]^-$, $[\text{EuCl}_4]^{2-}$, and $[\text{EuCl}_5]^{2-}$ complexes.

| System | EMI^+ | TCA^- | Cl^- | IL |
|-------------------------------------|----------------|----------------|---------------|---------------|
| | | | | |
| | | | | IL_1 |
| $[\text{UO}_2\text{Cl}_3]^-$ | -698 (10) | 230 (9) | 356 (9) | -112 (9) |
| $[\text{UO}_2\text{Cl}_4]^{2-}$ | -1340 (20) | 524 (11) | 559 (15) | -257 (15) |
| $[\text{Eu}^{\text{IIICl}_4}]^{2-}$ | -717 (7) | 233 (8) | 341 (11) | -142 (9) |
| $[\text{Eu}^{\text{IIICl}_6}]^{4+}$ | -2877 (30) | 820 (26) | 917 (30) | -838 (23) |
| $[\text{Eu}^{\text{IIICl}_4}]^-$ | -712 (9) | 215 (11) | 339 (9) | -158 (11) |
| $[\text{Eu}^{\text{IIICl}_5}]^{2-}$ | -1349 (16) | 531 (12) | 554 (16) | -263 (14) |
| $[\text{Eu}^{\text{IIICl}_6}]^{3-}$ | -2146 (27) | 620 (14) | 1082 (33) | -487 (17) |
| | | | | IL_3 |
| $[\text{UO}_2\text{Cl}_3]^-$ | -1389 (18) | 230 (13) | 915 (19) | -243 (13) |
| $[\text{Eu}^{\text{IIICl}_3}]^-$ | -667 (12) | 168 (10) | 353 (11) | -146 (12) |
| $[\text{Eu}^{\text{IIICl}_5}]^{3-}$ | -2016 (34) | 397 (21) | 1120 (35) | -499 (19) |
| $[\text{Eu}^{\text{IIICl}_6}]^{4+}$ | -2845 (37) | 627 (19) | 1082 (33) | -833 (21) |
| $[\text{Eu}^{\text{IIICl}_4}]^-$ | -634 (16) | 150 (17) | 334 (23) | -152 (12) |
| $[\text{Eu}^{\text{IIICl}_5}]^{3-}$ | -2146 (24) | 395 (11) | 1272 (21) | -480 (17) |

$[\text{EuCl}_5(\text{tca})]^{3-}$ species. In none of these simulations did the commonly observed $[\text{EuCl}_6]^{3-}$ complex spontaneously form.

In the more basic IL_3 liquid, simulation of one Eu^{3+} ion for 2 ns did not lead to the formation of $[\text{EuCl}_6]^{3-}$ either, but only to $[\text{EuCl}_4(\text{tca})_2]^{3-}$. Simulation of a more concentrated system with nine Eu^{3+} ions for 2 ns led to a mixture of one $[\text{EuCl}_4(\text{tca})_2]^{3-}$, five $[\text{EuCl}_5(\text{tca})]^{3-}$, and three $[\text{EuCl}_6]^{3-}$ species. There is thus no strong driving force for the formation of $[\text{EuCl}_6]^{3-}$. On the other hand, when a model of this complex was built and simulated for 2 ns in the IL_1 and IL_3 liquids, it did not dissociate. It is thus important to compare the solvation of the different chloro complexes, as well as their intrinsic stability.

In the gas phase, according to QM optimization at the HF or DFT levels, the octahedral $[\text{EuCl}_6]^{3-}$ structure corresponds to a local energy minimum, but is unstable towards the dissociation of one or two Cl^- ligands, resulting in the formation of the $[\text{EuCl}_5]^{2-}$ and $[\text{EuCl}_4]^-$ species (see Figure 6).^[25] A similar conclusion has been obtained by MD simulations in the gas phase with two electrostatic models ($q_{\text{Eu}} = 3.0 \text{ e}$ or 1.5 e with Cl charges adjusted accordingly), as well as with two Cl models;^[25] this suggests that the $[\text{EuCl}_6]^{3-}$ complex, if observed, is stabilized by its environment (e.g., counterions, solvent). Interestingly, according to the MD results, when transferred from the gas phase into the liquid, $[\text{EuCl}_6]^{3-}$ gains in internal stability (by $\approx 10 \text{ kcal mol}^{-1}$), because its Eu–Cl bonds shorten somewhat (by $\approx 0.05 \text{ \AA}$).

In the gas phase, the $[\text{EuCl}_4(\text{tca})_2]^{3-}$ complex was also calculated to be unstable. QM “optimizations” were performed at the HF and DFT levels, starting with two different structures. The first structure was extracted from the IL_1 liquid simulation (the two TCA^- ions are monodentate with a *cis* relationship), while the second one was modeled with *trans* TCA^- ions. In fact, both structures lost their two TCA^- ions to form a tetrahedral $[\text{EuCl}_4]^-$ species. These results are consistent with the lack of affinity of $[\text{EuCl}_4]^-$ for Cl^- ions in the gas phase, as mentioned above. An AMBER MD simulation of $[\text{EuCl}_4(\text{tca})_2]^{3-}$ in the gas phase also led to the rapid dissociation of one TCA^- ion. The $[\text{EuCl}_5(\text{tca})]^{3-}$ complex was also found to lose its TCA^- ion during QM energy minimization in the gas phase, which again hints at important solvation effects in the ionic liquid solution.

The importance of the solvent effect was supported by analysis of the solute–solvent interactions energies of the $[\text{EuCl}_4(\text{tca})_2]^{3-}$, $[\text{EuCl}_5(\text{tca})]^{3-}$, and $[\text{EuCl}_6]^{3-}$ complexes in the IL_1 liquid, which revealed (Tables 3 and 5) increased stabilizing contributions in this series:

- 1) The interaction of these -3 charged complexes with the solvent (from ≈ -415 to $-490 \text{ kcal mol}^{-1}$), mainly due to the contribution of the EMI^+ ions.
- 2) The interaction of Eu^{3+} with the whole surrounding medium, that is, coordinated ions as well as solvent ions (from ≈ -1100 to $-1210 \text{ kcal mol}^{-1}$).
- 3) The interaction of the chloro moiety of these complexes (i.e. $[\text{EuCl}_4]^-$, $[\text{EuCl}_5]^{2-}$, and $[\text{EuCl}_6]^{3-}$) with its whole environment, including first-shell TCA^- ions for the first two complexes (from ≈ -160 to $-490 \text{ kcal mol}^{-1}$).

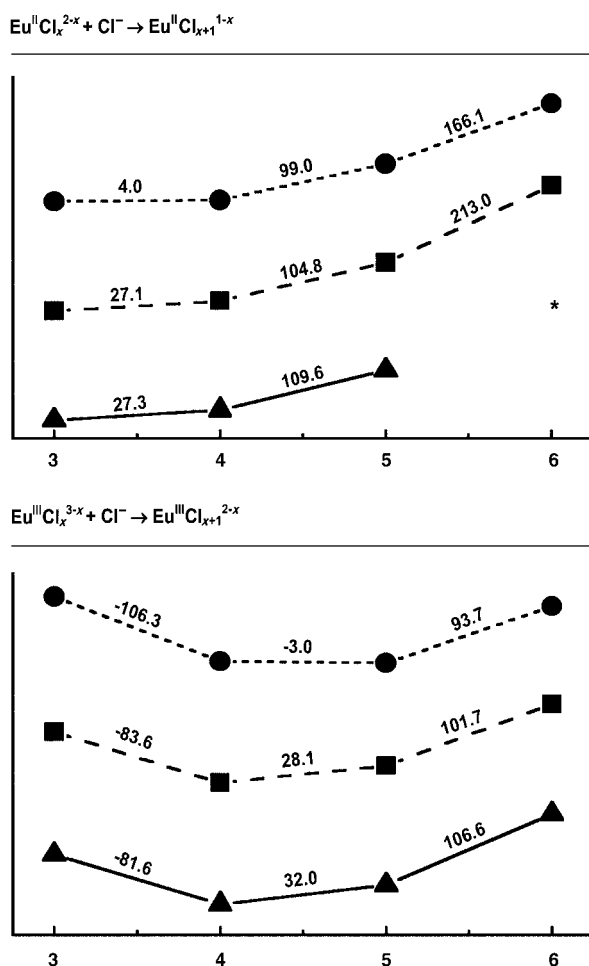


Figure 6. Eu^{2+} and Eu^{3+} chloro complexes in the gas phase: energy changes [kcal mol⁻¹] upon complexation of Cl^- , as obtained by molecular mechanics (●), HF (6-31+G*; ■) and DFT (B3LYP/6-31+G*; ▲) calculations. *: $[\text{EuCl}_6]^{4-}$ decomposes during the geometry optimization.

We notice that the better solvation of $[\text{EuCl}_6]^{3-}$, relative to $[\text{EuCl}_5]^{2-}$ ($\Delta_{\text{solv}} \approx 230 \text{ kcal mol}^{-1}$), largely compensates for the intrinsic (“gas phase”) lower stability of $[\text{EuCl}_6]^{3-}$ ($\Delta_{\text{gas}} \approx 100 \text{ kcal mol}^{-1}$, according to QM or force field results).

A similar comparison of $[\text{EuCl}_6]^{3-}$ and $[\text{EuCl}_4(\text{tca})_2]^{3-}$ complexes in the IL_1 and IL_3 solutions also shows (see Table 3) that $[\text{EuCl}_6]^{3-}$ interacts better with the solvent than its less halogenated analogue does (by $\approx 30 \text{ kcal mol}^{-1}$ in IL_1 and 75 kcal mol^{-1} in IL_3), and that the Eu^{3+} ion in $[\text{EuCl}_6]^{3-}$ again interacts with its whole environment better than that in the $[\text{EuCl}_4(\text{tca})_2]^{3-}$ complex (by $\approx 100 \text{ kcal mol}^{-1}$ in IL_1 and $130 \text{ kcal mol}^{-1}$ in IL_3). On the other hand, $[\text{EuCl}_4(\text{tca})_2]^{3-}$, which dissociated in the gas phase, is strongly attracted to the solvent ($\approx -400 \text{ kcal mol}^{-1}$). When compared to these gas-phase results, the MD results in solution show the importance of second-shell and remote solvent interactions in stabilizing complexes such as $[\text{EuCl}_4(\text{tca})_2]^{2-}$ or $[\text{EuCl}_6]^{3-}$.^[50]

Comparison of the solvation of $[\text{EuCl}_6]^{3-}$ in the IL_1 and IL_3 liquids shows striking similarities. As seen from the RDFs and snapshots of the solvation shells (see Figures 5

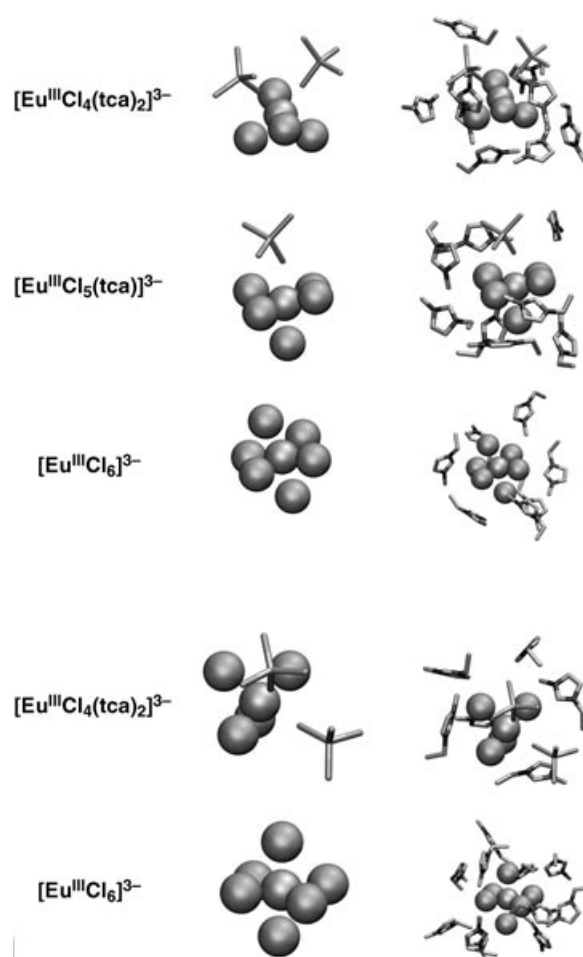


Figure 7. Eu^{3+} in IL_1 (top three rows) and IL_3 (bottom two rows) solutions: snapshots of the first solvation shell with anions only (left) and with anions + cations (right).

and 7), the complex is surrounded by a “cage” of EMI^+ ions, some of which form $\text{C}_2\text{H}\cdots\text{Cl}$ hydrogen bonds with the first-shell chlorides, as observed in the neat liquids. The interaction energies of the complexed Eu^{3+} ion with the two liquids (involving the first shell chlorides) are remarkably similar: they differ by 4 kcal mol^{-1} only (see Table 3).^[51]

The europium(III) cation in the basic liquids: When simulated in the IL_1 liquid, the divalent Eu^{2+} ion formed an $[\text{EuCl}_3(\text{tca})_3]^{4-}$ complex that remained stable for 4 ns of dynamics. A subsequent mixing–demixing simulation led first to the formation of $[\text{EuCl}_4(\text{tca})]^{3-}$ and, after 0.45 ns, to $[\text{EuCl}_4(\text{tca})_2]^{4-}$. The TCA⁻ ions are monodentate in these two complexes, giving total coordination numbers of five and six, respectively, for europium. Simulation of a concentrated solution (with nine Eu^{2+} ions) led after 2 ns to a mixture of four $[\text{EuCl}_4(\text{tca})_2]^{4-}$, four $[\text{EuCl}_3(\text{tca})_3]^{4-}$, and one $[\text{EuCl}_2(\text{tca})_4]^{4-}$ complexes.

In the “dilute” IL_3 solution, Eu^{2+} also formed an $[\text{EuCl}_3(\text{tca})_3]^{4-}$ complex, while the mixing–demixing simulation led to $[\text{EuCl}_3]^{3-}$. In the more concentrated IL_3 solution (with nine Eu^{2+} ions), three $[\text{EuCl}_3(\text{tca})_3]^{4-}$, four $[\text{Eu}$

$\text{Cl}_4(\text{tca})_2]^{4-}$, one $[\text{EuCl}_5(\text{tca})]^{4-}$, and one $[\text{EuCl}_6]^{4-}$ complexes were found after 2 ns of a “standard” simulation, while a subsequent mixing–demixing simulation led to a mixture of one $[\text{EuCl}_3(\text{tca})_3]^{4-}$, two $[\text{EuCl}_4(\text{tca})_2]^{4-}$, five $[\text{EuCl}_5(\text{tca})]^{4-}$, and one $[\text{EuCl}_6]^{4-}$ complexes. Only in two cases did the $[\text{EuCl}_6]^{4-}$ complex form spontaneously. However, when the latter was simulated for 1.5 ns in IL_1 and in IL_3 solutions, it did not dissociate. According to an energy component analysis, $[\text{EuCl}_6]^{4-}$ has stronger attractions with the IL_1 liquid than $[\text{EuCl}_4(\text{tca})_2]^{4-}$ ($\Delta E_{\text{sol}} \approx 170 \text{ kcal mol}^{-1}$), and stronger interactions with the IL_3 liquid than $[\text{EuCl}_3(\text{tca})_3]^{4-}$ ($\Delta E_{\text{sol}} \approx 180 \text{ kcal mol}^{-1}$).

The $[\text{EuCl}_6]^{4-}$ complex is intrinsically unstable (i.e., in the gas phase) and should dissociate to smaller complexes. The DFT calculations on this complex did not converge, while according to QM and force-field calculations (Figure 6), it should lose up to three Cl^- ions in the gas phase, that is, dissociate to $[\text{EuCl}_3]^-$.^[52,53] It is important to note that the intrinsic energy loss ΔE_{gas} upon dissociation of Cl^- ions is more than compensated by the gain in “interaction energy” ΔE_{sol} with the liquid. Compare for instance the dissociation of $[\text{EuCl}_6]^{4-}$ to $[\text{EuCl}_4]^{2-}$ in IL_1 ($\Delta E_{\text{sol}} \approx 700 \text{ kcal mol}^{-1}$, $\Delta E_{\text{gas}} \approx -300 \text{ kcal mol}^{-1}$), or the dissociation of $[\text{EuCl}_6]^{4-}$ to $[\text{EuCl}_5]^{3-}$ in IL_3 ($\Delta E_{\text{sol}} \approx 300 \text{ kcal mol}^{-1}$, $\Delta E_{\text{gas}} \approx -200 \text{ kcal mol}^{-1}$).

The solvation of the $[\text{EuCl}_6]^{4-}$ complex qualitatively looks the same in the IL_1 and IL_3 solutions (see RDFs in Figure 5 and snapshots of the first solvation shell in Figure 8). In both liquids the complex is surrounded by a cage of about 15 EMI^+ ions within 10 Å of Eu^{II} , which corresponds to a broad peak in the $\text{Eu} \cdots \text{EMI}^+$ RDFs. The resulting field clearly stabilizes the inserted anionic complexes.

$[\text{Eu}^{\text{III}}(\text{H}_2\text{O})_8]$ in the basic IL_1 and IL_3 ionic liquids, and in the neutral $[\text{EMI}][\text{TCA}]$ liquid: As the simulated ionic liquids and the lanthanide cations are highly hygroscopic, we decided to test the stability and solvation of the hydrated $[\text{Eu}(\text{H}_2\text{O})_8]^{3+}$ complex immersed in the IL_1 and IL_3 solutions by performing MD simulations for 5 ns at 400 K. For comparison, $[\text{Eu}(\text{H}_2\text{O})_8]^{3+}$ was also simulated in the “neutral” $[\text{EMI}][\text{TCA}]$ liquid. Typical RDFs and snapshots of the first solvation shell of Eu^{3+} are given in Figure 9.

During the dynamics in the IL_1 liquid, two H_2O molecules rapidly exchanged with Cl^- ions from the liquid to form the $[\text{EuCl}_2(\text{H}_2\text{O})_6]^{+}$ complex, whose six water molecules are hydrogen bonded to “second shell” solvent anions. Performing the dynamics for up to 2 ns resulted in the capture of another Cl^- ion to give the neutral $[\text{EuCl}_3(\text{H}_2\text{O})_4]$ species, while one H_2O moved into the second shell and the other three “free” H_2O molecules diffused into the bulk liquid, to about 10 Å from the complex. The neutral $[\text{EuCl}_3(\text{H}_2\text{O})_4]$ complex remained stable until the end of the dynamics. Analysis of the two first shells shows that the cation is surrounded by a total of five (4+1) H_2O and eight (3+5) Cl^- species, but no TCA^- ions. The relay of hydrogen-bonding interactions with water may explain why, in spite of the larger affinity of Eu^{3+} for Cl^- than for H_2O , no further coordination of Cl^- to Eu^{3+} takes place. In addition, the negatively charged aggregate is embedded in a “shell” of about eight EMI^+ ions.

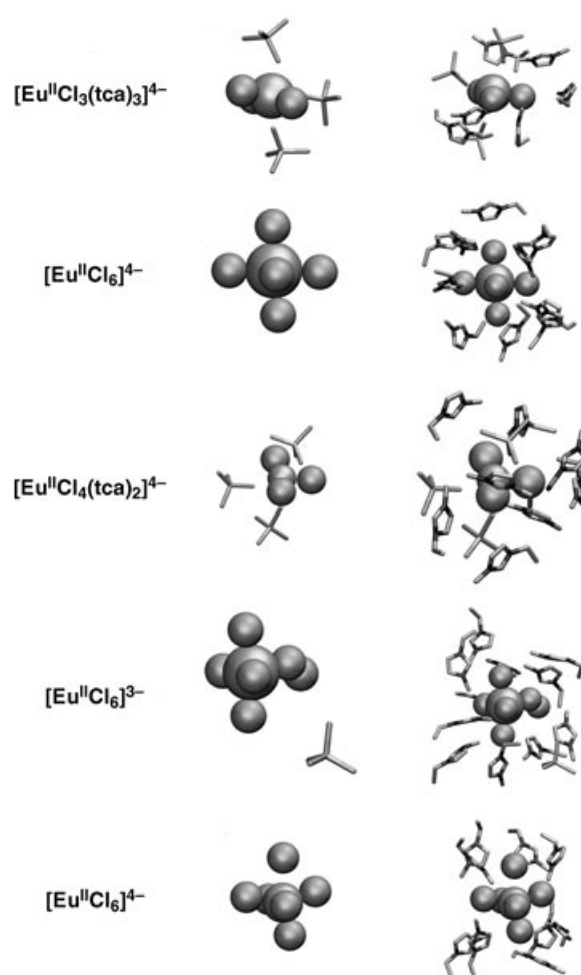


Figure 8. Eu^{2+} in IL_1 (top two rows) and IL_3 (bottom three rows) solutions: snapshots of the first solvation shell with anions only (left) and with anions + cations (right).

In the IL_3 liquid, the $[\text{Eu}(\text{H}_2\text{O})_8]^{3+}$ complex also exchanged first-shell water molecules with Cl^- ions, leading successively to $[\text{EuCl}_2(\text{H}_2\text{O})_6]^{+}$ (within 0.1 ns), $[\text{EuCl}_3(\text{H}_2\text{O})_4]$ (at 3.6 ns), and $[\text{EuCl}_4(\text{H}_2\text{O})_3]^-$ (at 4.3 ns), which remained stable until the end of the simulation (5 ns). Finally, two H_2O molecules diffused into the bulk liquid, while other three stayed in the second solvation shell, hydrogen-bonded to first-shell Cl^- ions. Thus, when compared with the results obtained in the IL_1 basic liquid, these results are consistent with the Le Chatelier rule, according to which an increased concentration of the Cl^- ion leads to a more halogenated complex. However, analysis of the first and second solvation shells of europium shows the same number (8 = 4 + 4) of Cl^- ions in IL_3 as in IL_1 ; this also leads to a -5 charged aggregate surrounded by a cationic solvent cage.

In both basic liquids, each “free” H_2O molecule displays bridging interactions with two solvent Cl^- ions on one side, and with two EMI^+ ions on the other side (see RDFs and snapshots in Figure 10). The bridging hydrogen bonds in the “bulk” liquids correspond to short $\text{Cl}^- \cdots \text{Cl}^-$ contacts (3–3.5 Å), reminiscent of patterns found in solid-state structures and by QM calculations in the gas phase.^[54]

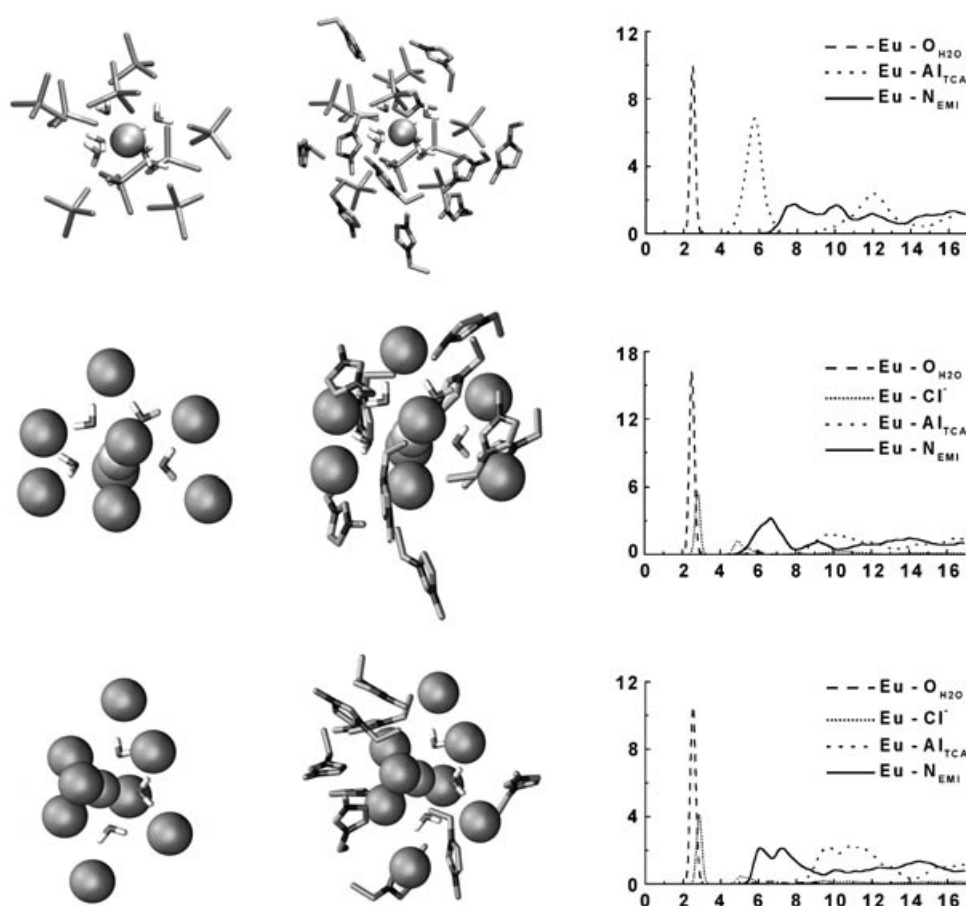


Figure 9. $[\text{Eu}(\text{H}_2\text{O})_8]^{3+}$ in neutral $[\text{EMI}][\text{TCA}]$ (top), basic IL_1 (middle) and IL_3 (bottom) solutions. From left to right: final snapshots of the first solvation shell of Eu^{3+} with anions + water only, with anions + cations + water, and $\text{Eu}-\text{Al}_{\text{TCA}}$, $\text{Eu}-\text{Cl}^-$, $\text{Eu}-\text{OH}_2$, and $\text{Eu}-\text{N}_{\text{EMI}}$ RDFs calculated over the last 200 ps.

The results obtained in the two basic liquids contrast with those obtained in the neutral $[\text{EMI}][\text{TCA}]$ analogue, in which the eight H_2O molecules remain coordinated in the first solvation shell of the metal without exchanging with TCA^- solvent ions within 1.5 ns. We notice the analogy between the cationic environment in this neutral liquid and in the solid-state structure of lanthanide(III) nonahydrates with weakly coordinating counterions like CF_3SO_3^- .^[55,56]

Discussion and Conclusions

We have reported here a theoretical investigation of the structures of two basic IL_1 and IL_3 ionic liquids based on EMI^+ and TCA^- ions, with different amounts of Cl^- . The results show the importance of the Cl^- ions, which display significant hydrogen-bonding-type interactions with the imidazolium solvent cations. Three cations, UO_2^{2+} , Eu^{3+} , and Eu^{2+} , were immersed in the liquids, and their solvation was investigated. In all cases, they were surrounded by solvent anions, with the contribution of the Cl^- anions dominating in the basic melts. In the two basic liquids, there is a strong tendency for the UO_2^{2+} ion to form the “saturated” $[\text{UO}_2\text{Cl}_4]^{2-}$ complex, which is commonly found in solid-state structures of imidazolium salts^[57,58] and in ionic liquid solu-

tions.^[4,59–64] According to our simulations in solution, this complex is stable and interacts more strongly with the ionic liquids than the mixed complexes do (e.g., $[\text{UO}_2\text{Cl}_3(\text{tca})]^{2-}$).

For the Eu^{3+} and Eu^{2+} ions, the situation is less clear cut, as the hexachloro $[\text{Eu}^{\text{III}}\text{Cl}_6]^{3-}$ and $[\text{Eu}^{\text{II}}\text{Cl}_6]^{4-}$ complexes rarely form spontaneously during the dynamics. To our knowledge, no mixed complexes involving lanthanide(III) cations have been identified so far, while their hexachloro complexes are common. For instance, $[\text{Eu}^{\text{III}}\text{Cl}_6]^{3-}$ and $[\text{Ce}^{\text{III}}\text{Cl}_6]^{3-}$ have been characterized in room-temperature basic ionic liquids based on aluminium chloride/imidazolium chloride salts.^[8,65] The $[\text{Nd}^{\text{III}}\text{Cl}_6]^{3-}$ complex similarly forms in ionic liquids composed of aluminium chloride and pyridinium or imidazolium chloride,^[66] as well as in binary melts based on $\text{NdCl}_3\text{-MCl}$ ($\text{M}=\text{Li}, \text{Na}, \text{K}, \text{Cs}$) mixtures at high temperatures.^[67] $[\text{LnCl}_6]^{3-}$ complexes have also been prepared in aprotic (e.g., acetoni-

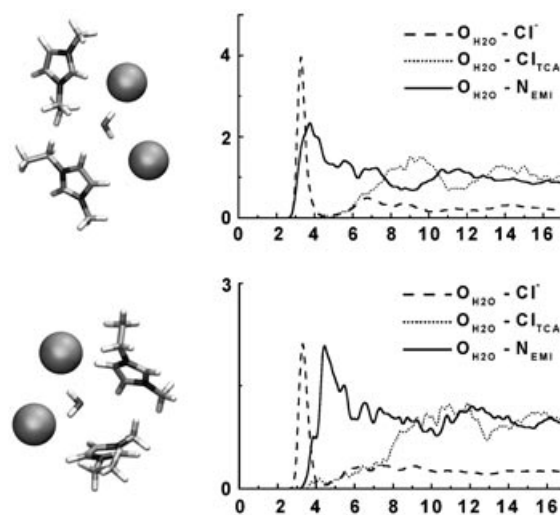


Figure 10. Environment of the “free” H_2O molecules of the $[\text{Eu}(\text{H}_2\text{O})_8]^{3+}$ system in basic IL_1 (top) and IL_3 (bottom) solutions: typical snapshots (left) and RDFs around $\text{O}_{\text{H}_2\text{O}}$ (right).

trile, succinonitrile)^[68] or in ethanolic solutions,^[69] as well as in the solid state with ammonium, imidazolium, or pyridinium counterions.^[70] Despite the frequent occurrence of hexachloro Ln^{III} complexes, it is important to note that, accord-

ing to the QM and force field calculations in the gas phase, they are metastable and should dissociate to less chlorinated species. This contrasts with the ionic liquid solutions in which these Ln^{III} complexes are stabilized by solvation forces.

The $[\text{Eu}^{\text{II}}\text{Cl}_6]^{4-}$ species is similarly predicted to dissociate in the gas phase, but also to be stabilized more by the ionic liquid than the less halogenated analogues. We find an equilibrium exists between tri- to hexachloro- Eu^{II} complexes, whose first shell is completed by TCA^- ions. The rare occurrence of $[\text{Eu}^{\text{II}}\text{Cl}_6]^{4-}$ and $[\text{Eu}^{\text{III}}\text{Cl}_6]^{3-}$ in our simulations may be due to 1) the slow diffusion of Cl^- anions, 2) the lack of an electrostatic driving force for negatively charged $[\text{Eu}^{\text{III}}\text{Cl}_n]^{3-n}$ or $[\text{Eu}^{\text{II}}\text{Cl}_n]^{2-n}$ ($n=4$ or 5) species to attract other Cl^- anions from the solvent, and 3) the first-shell Cl^-/TCA^- ion-exchange mechanism, which seems to involve crossing of the first imidazolium shell around the metal. The high viscosity of ionic liquids has also been mentioned experimentally as a possible source of hindrance for Eu^{II} complexation by macrocyclic ligands.^[24] The long lifetime (the half-life is ≈ 8 days) of electro-generated species such as $[\text{Ce}^{\text{II}}\text{Cl}_6]^{2-}$ in basic ionic liquids is also consistent with their slow diffusion.^[8] However, according to another study,^[65] $[\text{Eu}^{\text{II}}\text{Cl}_4]^{2-}$ is the only electro-attractive species produced during the reduction of $[\text{Eu}^{\text{III}}\text{Cl}_6]^{3-}$. Interestingly, this is also the species that forms in our simulations in the IL_3 basic solution, but, according to the energy component analysis, it should be stabilized less by solvation than $[\text{Eu}^{\text{II}}\text{Cl}_6]^{4-}$. Of course, other energy contributions (e.g., solvent-solvent interactions, and entropy) also determine the solvation of the cation, and so no firm conclusion can be drawn concerning the precise composition of the europium complexes. In principle, free-energy profiles for Cl^- dissociation in solution could be obtained from PMF-type (PMF = potential of mean force) calculations,^[71] but these remain a challenge in the ionic liquids that have been studied, mainly due to hysteresis and sampling issues.

An insight into the effect of traces of water was obtained from the simulations of the hydrated Eu^{III} ion, which evolved to the $[\text{EuCl}_3(\text{H}_2\text{O})_4]$ complex in IL_1 and to $[\text{EuCl}_4(\text{H}_2\text{O})_3]^-$ in IL_3 . The two first shells of these complexes are stabilized by hydrogen-bonding interactions with H_2O molecules and by the surrounding cage of imidazolium cations. Because of computer time limitations, only one starting configuration was considered, which was simulated for up to 5 ns. It is, however, gratifying to find that the $[\text{EuCl}_4(\text{H}_2\text{O})_3]^-$ complex is also found in the solid-state structure of a pyridinium salt.^[72] It is thus clear that traces of water modify the first coordination shell of the metal; this may have drastic consequences on its luminescence properties.^[24,73] What happens in more humid conditions remains to be investigated.

On the computational side, it is important to comment on the force-field representation of the simulated systems, in particular on the hypothesis of pair-wise additive coulombic interactions with $+2$ or $+3$ charges on the metal. As shown by the QM calculations, there is indeed important charge transfer between the metal and the coordinated anions. For instance, according to a Mulliken population analysis of the

$[\text{UO}_2\text{Cl}_4]^{2-}$ and $[\text{EuCl}_6]^{3-}$ complexes, the $q_{(\text{UO}_2)}$ and $q_{(\text{Eu})}$ charges are $+0.501 e$ and $+1.548 e$, respectively (DFT/6-31G* calculations). Polarization effects are also important, especially in the interaction of the first coordination shell of europium or uranyl. As a first and simple approach we assume that the interactions are mainly coulombic and steric in nature and that the ion parameters fitted to the free energies of hydration can also be transferred to another polar medium. Explicit accounting of many-body and charge-transfer effects certainly needs to be developed; this may lead to fine tuning of the structure and dynamics of the liquids and solutes. However, there is reasonable agreement between the DFT or HF results and the force field results for Eu^{II} and Eu^{III} chloro complexes (see Figure 6). The preference for the coordination of the metal to Cl^- over TCA^- is also well accounted for by the force-field calculations. The fact that charge-transfer effects do not critically determine the nature and solvation of the complexes can be seen from simulations of the $[\text{Eu}^{\text{III}}\text{Cl}_6]^{3-}$ complex in the $[\text{EMI}][\text{TCA}]$ solution, in which the solvation patterns obtained with reduced charges on $\text{Eu}(+1.5 e)$ and $\text{Cl}(-0.75 e)$ were the same as those with the $\text{Eu}(+3 e)$ and $\text{Cl}(-1 e)$ charges.^[25] All these data support the view that the main interactions are coulombic and steric in nature, as inferred from the analysis of related X-ray structures.^[74] The sampling problem is also very important, and should not be overlooked, as shown by the comparison of the "standard" simulations of "diluted solutions" (with one cation per solvent box, that is, $\approx 0.05 \text{ mol L}^{-1}$), the subsequent mixing-demixing simulations, and the simulations of more concentrated solutions. In particular, the occurrence of $[\text{Eu}^{\text{III}}\text{Cl}_6]^{3-}$ and $[\text{Eu}^{\text{II}}\text{Cl}_6]^{4-}$ complexes may be limited by the local concentration of Cl^- ions, and by the lack of long-range Cl^- attractions with the mixed complexes, whose presence in solution cannot thus be precluded. We hope that the simulations will stimulate experimental investigation of the systems that have been studied.

Note added in proof

We recently calculated by QM (6-31+G* basis set on Cl and O atoms and large core ECPs on the U atom) the energies of stepwise chlorination of UO_2Cl_2 , to form the UO_2Cl_3^- and $\text{UO}_2\text{Cl}_4^{2-}$ complexes. The energies obtained by the HF (-79.0 and $+27.3 \text{ kcal mol}^{-1}$), DFT-B3LYP (-71.4 and $+47.4 \text{ kcal mol}^{-1}$) and molecular mechanics calculations (-99.0 and $+12.8 \text{ kcal mol}^{-1}$) show that $\text{UO}_2\text{Cl}_4^{2-}$ is intrinsically unstable towards the loss of one Cl^- anion in the gas phase. This strengthens our conclusions on the importance of solvation forces on the stabilization of the $\text{UO}_2\text{Cl}_4^{2-}$ complex.

Acknowledgements

The authors are grateful to IDRIS, CINES, Université Louis Pasteur, and PARIS for computer resources and to Etienne Engler for his kind assistance.

[1] P. Wasserscheid, T. Welton, *Ionic Liquids in Synthesis*, Wiley-VCH, Weinheim, 2002.

[2] K. R. Seddon, *J. Chem. Technol. Biotechnol.* 1997, 68, 351.

- [3] M. J. Earle, K. R. Seddon, *Pure Appl. Chem.* **2000**, *72*, 1391.
- [4] S. Dai, L. M. Toth, G. G. DelCul, D. H. Metcalf, *J. Phys. Chem.* **1996**, *100*, 220.
- [5] S. Dai, L. M. Toth, G. D. DelCul, D. H. Metcalf, *Inorg. Chem.* **1995**, *34*, 412.
- [6] J. P. Schöebrechts, B. Gilbert, *Inorg. Chem.* **1985**, *24*, 2105.
- [7] P. B. Hitchcock, K. R. Mohammed, K. R. Seddon, C. L. Hussey, E. H. Ward, *Inorg. Chim. Acta* **1986**, *113*, L25.
- [8] F. M. Lin, C. L. Hussey, *J. Electrochem. Soc.* **1993**, *140*, 3093.
- [9] T. Welton, *Chem. Rev.* **1999**, *99*, 2071.
- [10] D. A. Costa, W. H. Smith, H. J. Dewey in *Molten Salts XII* (Eds.: P. C. Trulove, H. C. DeLong, G. R. Stafford, S. Deki), The Electrochemical Society Proceedings Series, Pennington, NJ, **2000**, p. 1820.
- [11] A. E. Visser, R. D. Rogers, *J. Solid State Chem.* **2003**, *171*, 106.
- [12] A. E. Visser, M. P. Jensen, I. Laszak, K. L. Nash, G. Choppin, R. D. Rogers, *Inorg. Chem.* **2003**, *42*, 2197.
- [13] A. E. Visser, R. P. Swatloski, W. M. Reichert, R. Mayton, S. Sheff, A. Wierzbicki, J. Davies, R. D. Rogers, *Environ. Sci. Technol.* **2002**, *36*, 2523.
- [14] A. E. Visser, R. P. Swatloski, S. T. Griffin, D. H. Hartman, R. D. Rogers, *Sep. Sci. Technol.* **2001**, *36*, 785.
- [15] C. G. Hanke, S. L. Price, R. M. Lynden-Bell, *Mol. Phys.* **2001**, *99*, 801.
- [16] J. de Andrade, E. S. Böes, H. Stassen, *J. Phys. Chem. B* **2002**, *106*, 13344.
- [17] J. K. Shah, J. F. Brennecke, E. J. Maginn, *Green Chem.* **2002**, *4*, 112.
- [18] T. I. Morrow, E. J. Maginn, *J. Phys. Chem. B* **2002**, *106*, 12807.
- [19] C. G. Hanke, N. A. Atamas, R. M. Lynden-Bell, *Green Chem.* **2002**, *4*, 107.
- [20] C. G. Hanke, A. Johansson, J. B. Harper, R. M. Lynden-Bell, *Chem. Phys. Lett.* **2003**, *374*, 85.
- [21] C. G. Hanke, R. M. Lynden-Bell, *J. Phys. Chem. B* **2003**, *107*, 10873.
- [22] A. Chaumont, E. Engler, G. Wipff, *Inorg. Chem.* **2003**, *42*, 5348.
- [23] A. Chaumont, G. Wipff, *Phys. Chem. Chem. Phys.* **2003**, *5*, 3481.
- [24] I. Billard, G. Moutiers, A. Labet, A. ElAzzi, C. Gaillard, C. Mariet, K. Lutzenkirchen, *Inorg. Chem.* **2003**, *42*, 1726.
- [25] A. Chaumont, G. Wipff, *J. Phys. Chem. A* **2004**, *108*, 3311.
- [26] D. A. Case, D. A. Pearlman, J. C. Caldwell, T. E. Cheatham III, W. S. Ross, C. L. Simmerling, T. A. Darden, K. M. Merz, R. V. Stanton, A. L. Cheng, J. J. Vincent, M. Crowley, D. M. Ferguson, R. J. Radmer, G. L. Seibel, U. C. Singh, P. K. Weiner, P. A. Kollman, AMBER 5.0, University of California, San Francisco, **1997**.
- [27] P. Guilbaud, G. Wipff, *J. Mol. Struct.* **1996**, *366*, 55.
- [28] F. C. J. M. van Veggel, D. Reinhoudt, *Chem. [Eur. J.]* **1999**, *5*, 90.
- [29] J. Åqvist, *J. Phys. Chem.* **1990**, *94*, 8021.
- [30] R. D. Shannon, *Acta Crystallogr. Sect. A* **1976**, *32*, 751.
- [31] G. Moreau, R. Scopelliti, L. Helm, J. Purans, A. E. Merbach, *J. Phys. Chem. A* **2002**, *106*, 9612.
- [32] F. Berny, PhD Thesis, **2000**, Université Louis Pasteur, Strasbourg.
- [33] T. A. Darden, D. M. York, L. G. Pedersen, *J. Chem. Phys.* **1993**, *98*, 10089.
- [34] H. J. C. Berendsen, J. P. M. Postma, W. F. van Gunsteren, A. DiNola, *J. Chem. Phys.* **1984**, *81*, 3684.
- [35] E. Engler, G. Wipff, unpublished results.
- [36] I. G. Tironi, R. Sperb, P. E. Smith, W. F. van Gunsteren, *J. Chem. Phys.* **1995**, *102*, 5451.
- [37] W. Humphrey, A. Dalke, K. Schulten, *J. Mol. Graphics* **1996**, *14*, 33.
- [38] Gaussian 98 (Revision A.7), M. J. Frisch, G. W. Trucks, H. B. Schlegel, G. E. Scuseria, M. A. Robb, J. R. Cheeseman, V. G. Zakrzewski, J. A. Montgomery, Jr., R. E. Stratmann, J. C. Burant, S. Dapprich, J. M. Millam, A. D. Daniels, K. N. Kudin, M. C. Strain, O. Farkas, J. Tomasi, V. Barone, M. Cossi, R. Cammi, B. Mennucci, C. Pomelli, C. Adamo, S. Clifford, J. Ochterski, G. A. Petersson, P. Y. Ayala, Q. Cui, K. Morokuma, D. K. Malick, A. D. Rabuck, K. Raghavachari, J. B. Foresman, J. Cioslowski, J. V. Ortiz, B. B. Stefanov, G. Liu, A. Liashenko, P. Piskorz, I. Komaromi, R. Gomperts, R. L. Martin, D. J. Fox, T. Keith, M. A. Al-Laham, C. Y. Peng, A. Nanayakkara, C. Gonzalez, M. Challacombe, P. M. W. Gill, B. G. Johnson, W. Chen, M. W. Wong, J. L. Andres, M. Head-Gordon, E. S. Replogle, J. A. Pople, Gaussian, Inc., Pittsburgh, PA, **1998**.
- [39] J. V. Ortiz, P. J. Hay, R. L. Martin, *J. Am. Chem. Soc.* **1992**, *114*, 2736.
- [40] M. Dolg, H. Stoll, A. Savin, H. Preuss, *Theor. Chim. Acta* **1989**, *75*, 173.
- [41] M. Dolg, H. Stoll, A. Savin, H. Preuss, *Theor. Chim. Acta* **1993**, *85*, 441.
- [42] T. H. Dunning, P. J. Hay in *Methods of Electronic Structure Theory. Modern Theoretical Chemistry 3*, (Ed.: H. F. Schaefer III, Plenum Press, New York, **1977**, p. 1.
- [43] J. A. A. Fannin, D. A. Floreani, L. A. King, J. S. Landers, B. J. Piersma, D. J. Stech, R. L. Vaughn, J. S. Wilkes, J. L. Williams, *Chem. Phys.* **1984**, *88*, 2614.
- [44] S. Saha, S. Hayashi, A. Kobayashi, H. Hamaguchi, *Chem. Lett.* **2003**, *32*, 740.
- [45] E. A. Turner, C. C. Pye, R. D. Singer, *J. Phys. Chem. A* **2003**, *107*, 2277.
- [46] C. Hardacre, J. D. Holbrey, S. E. J. McMath, D. T. Browron, A. K. Soper, *J. Chem. Phys.* **2003**, *118*, 273.
- [47] J. H. Antony, D. Mertens, A. Dölle, P. Wasserscheid, W. R. Carper, *ChemPhysChem* **2003**, *4*, 588.
- [48] This is mainly due to the contribution of the Cl⁻ ions ($\Delta \approx -150$ kcal mol⁻¹), compensated by the loss of TCA⁻ interactions ($\Delta \approx 80$ kcal mol⁻¹) and by somewhat enhanced repulsions of the EMI⁺ cations ($\Delta = 40$ kcal mol⁻¹).
- [49] The loss of the interactions of uranyl with TCA⁻ ions observed when IL₃ is compared with IL₁ is compensated by enhanced uranyl interactions with Cl⁻ ions, while the repulsions with the EMI⁺ ions increase, leading to a somewhat better solvation of the complex by IL₁ ($\Delta = 10$ kcal mol⁻¹). This is not sufficient, however, to conclude that there is greater solubility of uranyl in IL₁ due to other energy contributions, such as changes in solvent–solvent interactions, and different entropy changes in the liquids.
- [50] It is also interesting to note that the structure of the [EuCl₄]⁻ moiety of the complex is not the same in solution (the Cl⁻ ions are “on the same side” due to the hindrance of the two *cis* TCA⁻ ligands) as in the gas phase (tetrahedral “least repulsion” arrangement), which induces an intrinsic destabilization that further favors [EuCl₆]³⁻ over [EuCl₄]⁻ in solution.
- [51] This is due to the compensation by the different contributions, as observed with the uranyl cation: the increased attractions to the Cl⁻ anion from IL₁ to IL₃ are compensated by diminished attractions to the TCA⁻ anions and enhanced repulsions by the EMI⁺ cations.
- [52] We notice that the dissociation reaction is much more exothermic with the Eu^{II} than with the Eu^{III}–chloro complexes due to the lower charge on the metal and longer Eu–Cl distances in the former. The MD averaged Eu–Cl bond distances increase from 2.85 Å in [Eu^{III}Cl₆]³⁻ to 3.05 Å in the [Eu^{II}Cl₄(tca)]³⁻ and [Eu^{II}Cl₆]⁴⁻ complexes. This leads to reduced metal–anion attractions and to strain relief in the first coordination shell of Eu^{II} compared with Eu^{III}.
- [53] In molecular-mechanics-optimized [Eu^{III}Cl₆]³⁻ and [Eu^{II}Cl₆]⁴⁻ complexes, the energies of the Eu–anion attractions are –2041 and –1232 kcal mol⁻¹, while the energies of the intra-shell repulsions are +1190 and +1090 kcal mol⁻¹, respectively, in the gas phase.
- [54] J. Gao, S. Boudon, G. Wipff, *J. Am. Chem. Soc.* **1991**, *113*, 9610.
- [55] C. J. Kepert, L. Weimin, B. W. Skelton, A. H. White, *Aust. J. Chem.* **1994**, *47*, 365.
- [56] A. Chatterjee, E. N. Maslen, K. Watson, *Acta Crystallogr. Sect. B* **1988**, *44*, 381.
- [57] D. Perry, D. P. Freyberg, A. Zalkin, *J. Inorg. Nucl. Chem.* **1980**, *42*, 243.
- [58] A. Zalkin, D. Perry, L. Tsao, D. Zhang, *Acta Crystallogr. Sect. C* **1983**, *39*, 1186.
- [59] P. B. Hitchcock, T. J. Mohammed, K. R. Seddon, J. A. Zora, C. L. Hussey, E. H. Ward, *Inorg. Chim. Acta* **1986**, *113*, L25.
- [60] H. G. Brittain, D. L. Perry, L. Tsao, *Spectrochim. Acta Part A* **1984**, *40*, 651.
- [61] F. meuris, L. Heerman, W. D’Olieslager, *J. Electrochem. Soc.* **1980**, *127*, 1294.
- [62] T. A. Hopkins, J. M. Berg, D. Costa, W. Smith, H. J. Dewey, *Inorg. Chem.* **2001**, *40*, 1820.
- [63] C. J. Anderson, G. R. Choppin, D. J. Pruet, D. Costa, W. Smith, *Radiochim. Acta* **1999**, *84*, 31.
- [64] S. Dai, Y. S. Shin, L. M. Toth, C. E. Barnes, *Inorg. Chem.* **1997**, *36*, 4900.

- [65] W. J. Gau, I. W. Sun, *J. Electrochem. Soc.* **1996**, *143*, 914.
- [66] M. Lipsztajn, R. A. Osteryoung, *Inorg. Chem.* **1985**, *24*, 716.
- [67] G. M. Photiadis, B. Borresen, G. N. Papatheodorou, *J. Chem. Soc. Faraday Trans.* **1998**, *94*, 2605.
- [68] J. L. Ryan, C. K. Jørgensen, *J. Phys. Chem.* **1966**, *70*, 2845.
- [69] C. Görlier-Walrand, N. D. Moitié-Neyt, Y. Beyens, J. C. Bünzli, *J. Chem. Phys.* **1982**, *77*, 2261.
- [70] See for example, $[\text{MCl}_6]^{3-}$ complexes with Refcodes UFAXAA (M=La), DAKJEE (M=Ho), DAKPIO (M=Er), DAKQAH (M=Tm), FOXTIV10 (M=Yb) in the Cambridge Structural Database "CSD".
- [71] W. L. Jørgensen, *Acc. Chem. Res.* **1989**, *22*, 184. Preliminary PMF results in the IL_3 solution indicate that the dissociation of one Cl^- anion from $[\text{Eu}^{\text{III}}\text{Cl}_6]^{3-}$ is unfavourable ($\Delta G \approx 10 \text{ kcal mol}^{-1}$). The subsequent dissociation of Cl^- from $[\text{Eu}^{\text{III}}\text{Cl}_5]^{2-}$ is also unfavourable ($\Delta G \approx 11 \text{ kcal mol}^{-1}$), thus confirming our conclusions on the stability of $[\text{Eu}^{\text{III}}\text{Cl}_6]^{3-}$ in IL solution (A. Chaumont, G. Wipff, unpublished results).
- [72] D. Mackenstedt, W. Urland, *Z. Anorg. Allg. Chem.* **1993**, *619*, 1393.
- [73] After submission of this paper, a very interesting paper appeared, which demonstrates the effect of water and chlorination on the luminescence properties of Eu^{III} in a room temperature ionic liquid: I. Billard, S. Mekki, C. Gaillard, P. Hesemann, G. Moutiers, C. Mariet, A. Labet, J.-C. G. Bünzli, *Eur. J. Inorg. Chem.* **2004**, 1190.
- [74] J. Fuller, R. T. Carlin, H. C. D. Long, D. Haworth, *J. Chem. Soc. Chem. Commun.* **1994**, 299.

Received: March 3, 2004

Published online: June 24, 2004